bioRxiv preprint doi: https://doi.org/10.1101/2023.02.01.526470; this version posted June 22, 2023. The copyright holder for this preprint (which was not certified by peer review) is the author/funder, who has granted bioRxiv a license to display the preprint in perpetuity. It is made available under aCC-BY-NC-ND 4.0 International license.

SUPPLEMENTARY INFORMATION

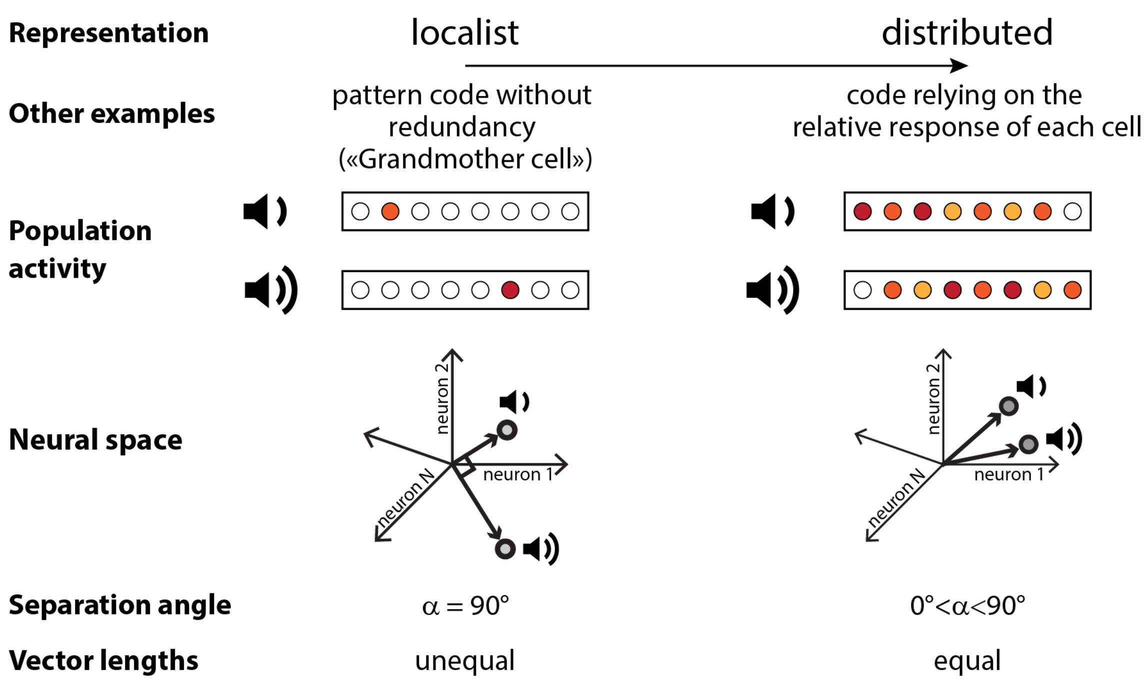

SUPPLEMENTARY FIGURE S1: ADDITIONAL EXAMPLES OF LOCALIST AND DISTRIBUTED REPRESENTATIONS

Localist versus distributed representations can be implemented in many ways. An example of localist code is the pattern code without redundancy (known as the “Grandmother cell”, (Bowers, 2009)). An example of distributed code is a code relying only on the relative response of each cell and not the magnitude of response of the population vector.

REFERENCE

Bowers, J.S., 2009. On the biological plausibility of grandmother cells: Implications for neural network theories in psychology and neuroscience. Psychological Review 116, 220–251. https://doi.org/10.1037/a0014462

bioRxiv preprint doi: https://doi.org/10.1101/2023.02.01.526470; this version posted June 22, 2023. The copyright holder for this preprint (which was not certified by peer review) is the author/funder, who has granted bioRxiv a license to display the preprint in perpetuity. It is made available under aCC-BY-NC-ND 4.0 International license.

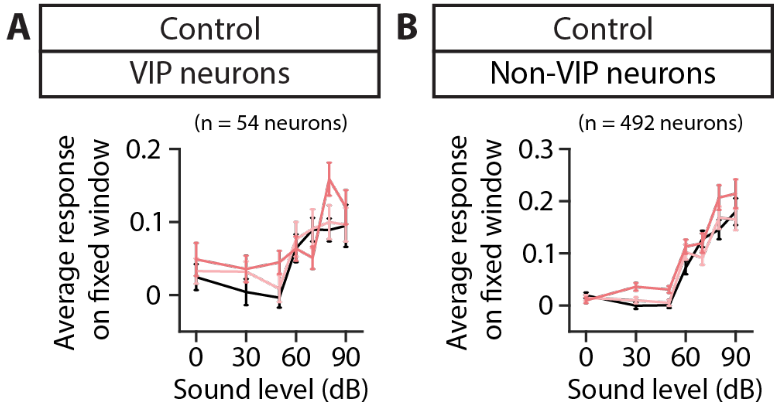

SUPPLEMENTARY FIGURE S2: CONTROL EXPERIMENT - LASER EFFECT IN THE ABSENCE OF AN OPTOGENETIC CHANNEL

A. Average fluorescence over a 1-s fixed window as a function of sound pressure level for the whole population of VIP neurons recorded, tagged with Flex.tdTomato, when the laser illuminates AC.

B. Average fluorescence over a 1-s fixed window as a function of sound pressure level for the whole population of neurons recorded (VIP neurons excluded) when the laser illuminates AC.

For all panels, black, pink and red colors correspond to no laser power (0 mW/mm2), medium laser power (~0.3 mW/mm2) and high laser power (~3.5 mW/mm2), respectively (see Methods for power calibration).

bioRxiv preprint doi: https://doi.org/10.1101/2023.02.01.526470; this version posted June 22, 2023. The copyright holder for this preprint (which was not certified by peer review) is the author/funder, who has granted bioRxiv a license to display the preprint in perpetuity. It is made available under aCC-BY-NC-ND 4.0 International license.

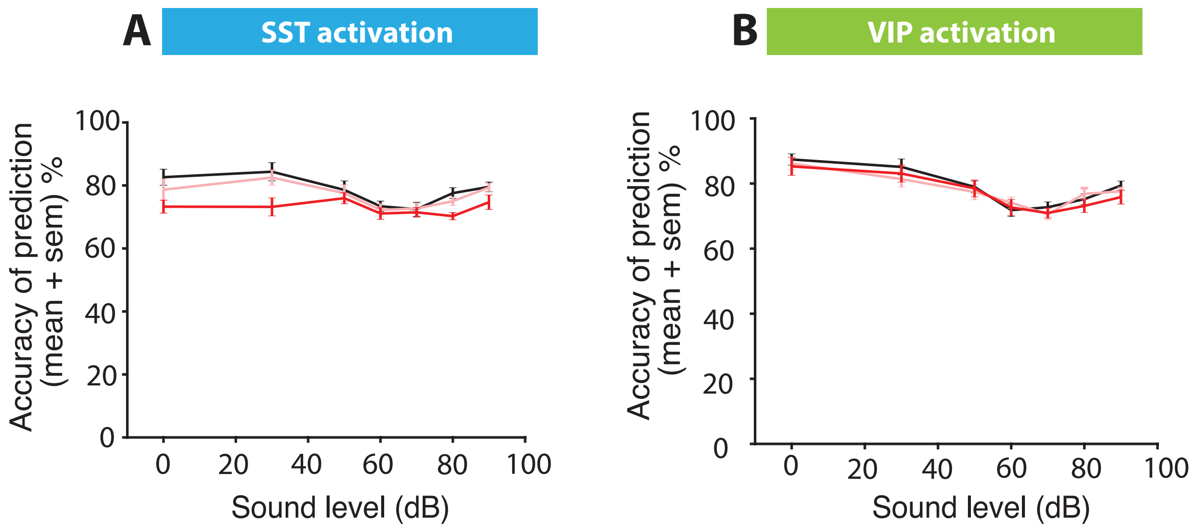

SUPPLEMENTARY FIGURE S3: DECODING ACCURACY OF SVM DECODER AT EACH LASER POWER

A. Decoding individual sound pressure levels using non-SST neuronal responses within 1-s fixed window, when the laser illuminates AC and stimulates SST neurons.

B. Decoding individual sound pressure levels using non-VIP neuronal responses within 1-s fixed window, when the laser illuminates AC and stimulates VIP neurons.

For all panels, black, pink and red colors correspond to no laser power (0 mW/mm2), medium laser power (~0.3 mW/mm2) and high laser power (~3.5 mW/mm2), respectively (see Methods for power calibration).

bioRxiv preprint doi: https://doi.org/10.1101/2023.02.01.526470; this version posted June 22, 2023. The copyright holder for this preprint (which was not certified by peer review) is the author/funder, who has granted bioRxiv a license to display the preprint in perpetuity. It is made available under aCC-BY-NC-ND 4.0 International license.

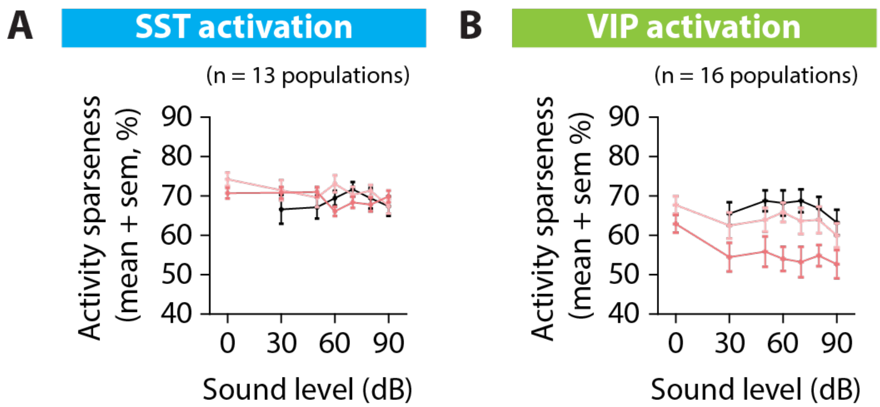

SUPPLEMENTARY FIGURE S4: ACTIVITY SPARSENESS MEASURED FROM SILENCE AND NO LASER

A. Average activity sparseness measured from silence and no laser as a function of sound pressure level for each population of neurons (SST neurons excluded), when the SST population is activated. There was no significant change in activity sparseness measured from silence and no laser upon SST activation (p_{laser}=0.11, GLME).

B. Average activity sparseness measured from silence and no laser as a function of sound pressure level for each population of neurons (VIP neurons excluded), when the VIP population is activated. There was a significant decrease in activity sparseness measured from silence and no laser upon VIP activation (***p_{laser}=4.9e-4, GLME).

The activity sparseness here was computed by subtracting each neuron's response over its optimal window to its response at 0dB and no laser power, and computing the ratio of neurons with an increase in response below threshold. The threshold was set as the standard deviation of the distribution of responses to 0dB and no laser power for each population. The point at 0dB for no laser power was by calculation 100% and thus omitted from the plot and the statistical test. For all panels, black, pink and red colors correspond to no laser power (0 mW/mm2), medium laser power (~0.3 mW/mm2) and high laser power (~3.5 mW/mm2), respectively (see Methods for power calibration).

bioRxiv preprint doi: https://doi.org/10.1101/2023.02.01.526470; this version posted June 22, 2023. The copyright holder for this preprint (which was not certified by peer review) is the author/funder, who has granted bioRxiv a license to display the preprint in perpetuity. It is made available under aCC-BY-NC-ND 4.0 International license.

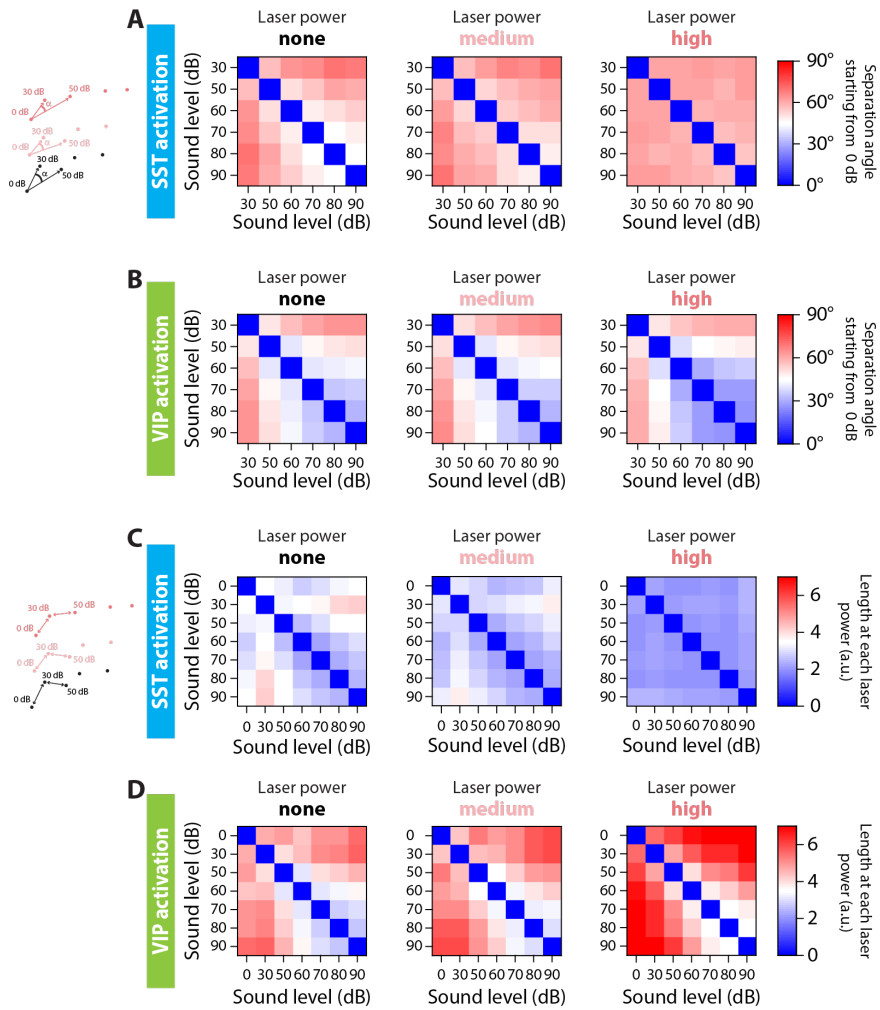

SUPPLEMENTARY FIGURE S5: CONFUSION MATRICES OF SEPARATION ANGLES AND VECTOR LENGTHS AT EACH LASER POWER

A. Confusion matrix of the separation angle between pairs of sound stimuli for no (left), medium (middle) and high (right) laser power of SST activation. Far left schematic: Low-dimensional schematic of the separation angle between mean population vectors to each sound pressure level at a given laser power, starting from 0dB at each laser power.

B. Confusion matrix of the separation angle between pairs of sound stimuli for no (left), medium (middle) and high (right) laser power of VIP activation.

C. Confusion matrix of the vector length between pairs of sound stimuli for no (left), medium (middle) and high (right) laser power of SST activation. Far left schematic: Low-dimensional schematic of the vector length of mean population vectors between sound pressure levels at a given laser power.

D. Confusion matrix of the vector length between pairs of sound stimuli for no (left), medium (middle) and high (right) laser power of VIP activation.

bioRxiv preprint doi: https://doi.org/10.1101/2023.02.01.526470; this version posted June 22, 2023. The copyright holder for this preprint (which was not certified by peer review) is the author/funder, who has granted bioRxiv a license to display the preprint in perpetuity. It is made available under aCC-BY-NC-ND 4.0 International license.

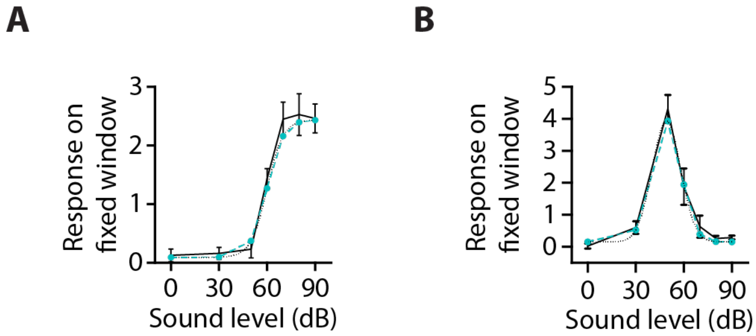

SUPPLEMENTARY FIGURE S6: COMPLETE FITTING PROCEDURE FOR MONOTONIC AND NONMONOTONIC CELLS

A. Example neuron with a monotonic response-level curve (solid black line) with a sigmoid fit estimated at the probed sound amplitudes (blue dashed line with circles) and the sigmoid function with the same parameters (dotted black line). The parameters for the sigmoid fit are: Offset amplitude $y_0 = 0.1$; Range $y_{range} = 2.3$; Midpoint $x_0 = 60$ dB; Width $\Delta x = 5$ dB.

B. Example neuron with a nonmonotonic response-level curve (solid black line) with a Gaussian fit estimated at the probed sound pressure levels (blue dashed line with circles) and the Gaussian function with the same parameters (dotted black line). The parameters for the Gaussian fit are: Offset amplitude $y_0 = 0.2$; Range $y_{range} = 3.8$; Mean $x_{mean} = 49$ dB; Standard Deviation $\sigma = 9$ dB.

bioRxiv preprint doi: https://doi.org/10.1101/2023.02.01.526470; this version posted June 22, 2023. The copyright holder for this preprint (which was not certified by peer review) is the author/funder, who has granted bioRxiv a license to display the preprint in perpetuity. It is made available under aCC-BY-NC-ND 4.0 International license.

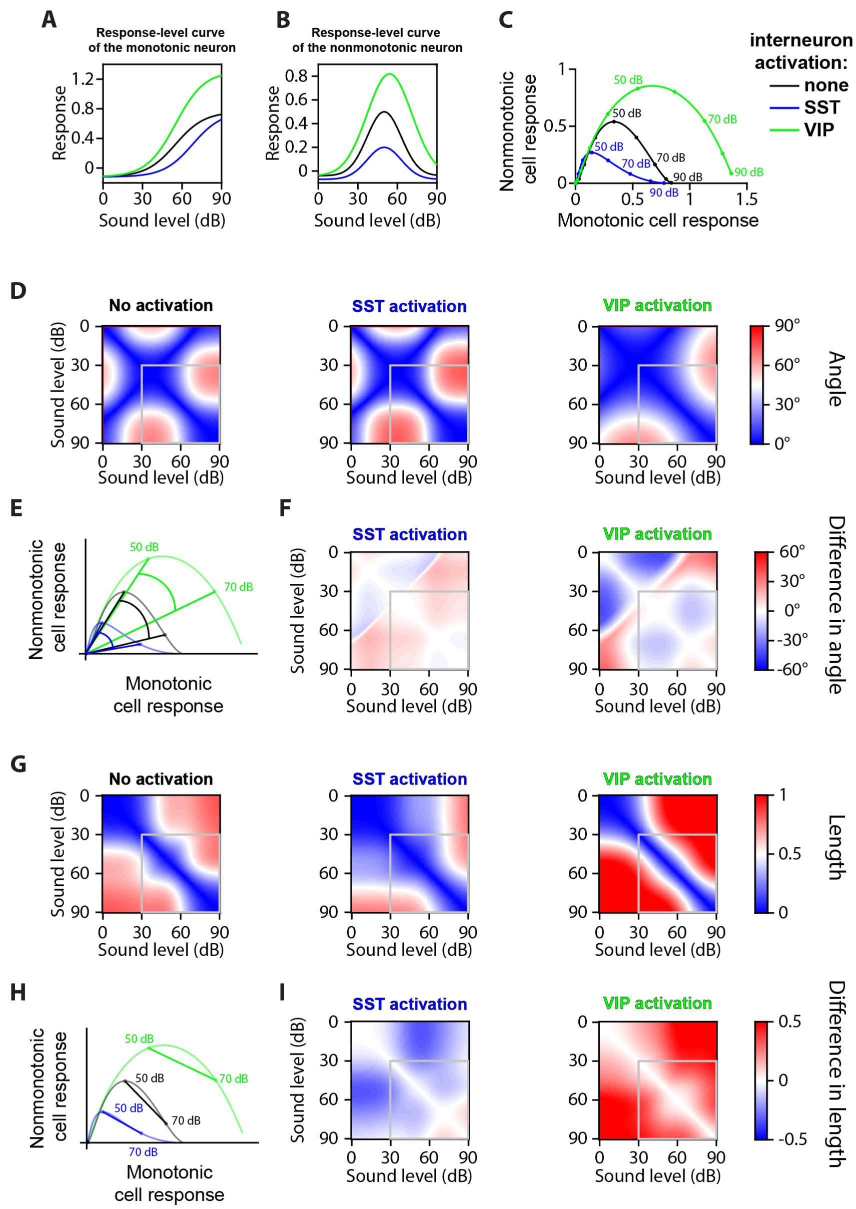

SUPPLEMENTARY FIGURE S7: TWO-CELL MODEL

A. Response-level curve of the monotonic cell with parameters taken as the mean parameters from Figure 5 at no and high laser power. Black indicates no interneuron activation, blue indicates SST activation and green indicates VIP activation. The parameters for the sigmoid curve with no interneuron activation (black) are: Offset amplitude y_0 = -0.12; Range y_{range} = 0.88; Midpoint x_0 = 55 dB; Width Δx = 11 dB. Upon SST activation (blue), all parameters remain constant except for: Midpoint x_0^{SST} = 68 dB; Upon VIP activation (green), all parameters remain constant except for: Range y_{range}^{VIP} = 1.43.

B. Response-level curve of the nonmonotonic cell with parameters taken as the mean parameters from Figure 6 at no and high laser power. Black indicates no interneuron activation, blue indicates

bioRxiv preprint doi: https://doi.org/10.1101/2023.02.01.526470; this version posted June 22, 2023. The copyright holder for this preprint (which was not certified by peer review) is the author/funder, who has granted bioRxiv a license to display the preprint in perpetuity. It is made available under aCC-BY-NC-ND 4.0 International license.

SST activation and green indicates VIP activation. The parameters for the Gaussian curve with no interneuron activation (black) are: Offset amplitude y_0 = -0.04; Range y_{range} = 0.54; Mean x_{mean} = 50 dB; Standard Deviation σ = 13 dB. Upon SST activation (blue), all parameters remain constant except for: Offset amplitude y_0^{SST} = -0.07; Range $y_{\text{range}}^{\text{SST}}$ = 0.27; Upon VIP activation (green), the offset amplitude remains constant, and: Range $y_{\text{range}}^{\text{VIP}}$ = 0.86; Mean x_{mean} = 54 dB; Standard Deviation σ = 17 dB.

C. Trajectory of the population's response from 0dB to 90dB in the neural space, with the response of the monotonic cell on the *x*-axis and the response of the nonmonotonic cell on the *y*-axis. The response of both cells at 0dB has been subtracted from the curves, thus the dots at the (0,0) coordinate are the response to 0dB, and the end of the curves on the right indicate the response to 90dB. The trajectories are computed from 0 dB to 90dB with 1dB increments, and circles on a line represent 10dB increments from 0dB to 90dB. Black indicates no interneuron activation, blue indicates SST activation and green indicates VIP activation.

D. Confusion matrix of the separation angle between population responses to each sound and laser power from silence at a given laser power, for no (left), SST (middle) and VIP (right) activation. Sound pressure level is in 1dB increments, and the gray box indicates the sound levels sampled in the experiments (Figure 4D and F, Supplementary Figure S3A-B)

E. Schematic in the neural space (see panel C) of the angle between 50 dB and 70dB when there is no (black), SST (blue) or VIP (green) activation, starting from the population's response to silence for each case of (or lack of) interneuron activation. The angle is greatest when SST neurons are activated, and smallest when VIP neurons are activated.

F. Confusion matrix of the difference in separation angle from SST (left) or VIP (right) activation to no interneuron activation, with the angles calculated as in (D). Sound level is in 1dB increments, and the gray box indicates the sound pressure levels sampled in the experiments (Figure 4D and F, Supplementary Figure S3A-B). The mean angle difference for SST activation is, over 1-90dB: + 3.6° and over 30-90dB: + 3.7°; for VIP activation, over 1-90dB: − 4.0°, and over 3-90dB: − 4.1°.

G. Confusion matrix of the length of the population vector between each sound pressure level at a given laser power, for no (left), SST (middle) and VIP (right) activation. Sound pressure level is in 1dB increments, and the gray box indicates the sound pressure levels sampled in the experiments (Figure 7I and K, Supplementary Figure S3C-D).

H. Schematic in the neural space (see panel C) of the vector length between 50 dB and 70dB when there is no (black), SST (blue) or VIP (green) activation. The vector length is greatest when VIP neurons are activated, and smallest when SST neurons are activated.

I. Confusion matrix of the difference in vector length from SST (left) or VIP (right) activation to no interneuron activation, with the lengths calculated as in (G). Sound pressure level is in 1dB increments, and the gray box indicates the sound pressure levels sampled in the experiments (Figure 7I and K, Supplementary Figure S3C-D). The mean length difference for SST activation is, over 1-90dB: − 0.12 a.u. and over 30-90dB: − 0.07 a.u.; for VIP activation, over 1-90dB, + 0.27 a.u. and over 30-90dB: + 0.21 a.u.

bioRxiv preprint doi: https://doi.org/10.1101/2023.02.01.526470; this version posted June 22, 2023. The copyright holder for this preprint (which was not certified by peer review) is the author/funder, who has granted bioRxiv a license to display the preprint in perpetuity. It is made available under aCC-BY-NC-ND 4.0 International license.

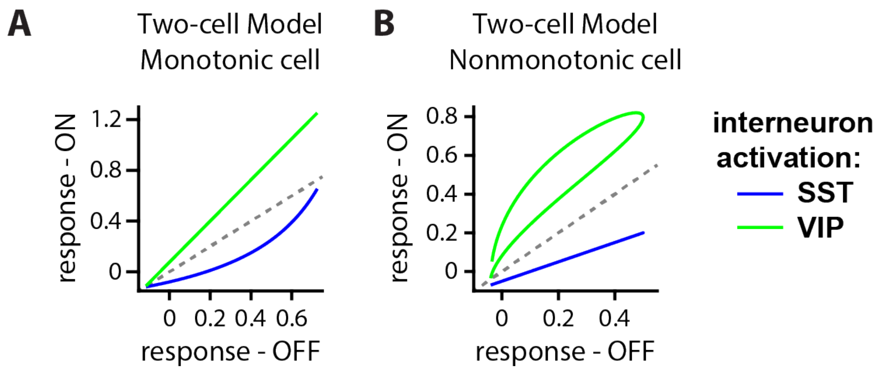

SUPPLEMENTARY FIGURE S8: NEURAL RESPONSE LASER ON VERSUS LASER OFF FOR THE MONOTONIC AND NONMONOTONIC CELL FROM THE TWO-CELL MODEL

A. Response of the monotonic cell with parameters taken as the mean parameters from Figure 5 (see Figure S5 for parameter values) with laser activation versus no laser activation. Blue indicates SST activation and green indicates VIP activation. SST activation shows a divisive regime, a subtractive regime, a combination of divisive and subtractive or multiplicative and subtractive regimes depending on the range of responses sampled. VIP activation shows a multiplicative regime or an additive and multiplicative regime depending on the range of responses sampled.

B. Response of the nonmonotonic cell with parameters taken as the mean parameters from Figure 6 (see Figure S5 for parameter values) with laser activation versus no laser activation. Blue indicates SST activation and green indicates VIP activation. SST activation shows a combination of divisive and subtractive regime. VIP activation shows a multiplicative regime, and additive regime or an additive and multiplicative regime depending on the range of responses sampled.

bioRxiv preprint doi: https://doi.org/10.1101/2023.02.01.526470; this version posted June 22, 2023. The copyright holder for this preprint (which was not certified by peer review) is the author/funder, who has granted bioRxiv a license to display the preprint in perpetuity. It is made available under aCC-BY-NC-ND 4.0 International license.

STATISTICS TABLE

We used a Generalized Linear Mixed-Effects (GLME) model and Wilcoxon signed-rank tests to compute the statistics for the data.
For Figure 2, Figure 3B,C,E,G,H, J; Figure S2, Figure S4, the data (‘`table`‘) had four columns: cell, sound level, laser power, output. The formula used was (Matlab):
`glme=fitglme(table,'output ~ sound + laser + sound*laser + (1|cell)');`
For Figure 3D,I, Figure 5 and Figure 6, the data (‘`table`‘) had three columns: cell, laser power, output. The formula used was (Matlab): `glme=fitglme(table,'output ~ laser + (1|cell)');`
For Figure 4D,F,H,G, the data (‘`table`‘) had four columns: cell, sound level difference, laser power, output. The formula used was (Matlab): `glme=fitglme(table,'output ~ sounddiff + laser + sounddiff*laser + (1|cell)');`
For Figure S3, we compared each sound amplitude across different light conditions using Wilcoxon tests.

Comparison	Figure	N	Test	Test Statistic	p-value	Effect size
FIGURE 2						
SST neuron with SST activation	Fig 2D	10 repeats	GLME	t_{laser}=7.89 t_{sound}=0.34 $t_{laser:sound}$=-0.55 DF = 206	***p_{laser}=1.8e-13** p_{sound}=0.74 $p_{laser:sound}$=0.58	η_{laser}^2=0.58 η_{sound}^2=3.8e-3 $\eta_{laser:sound}^2$=1.5e-2
Sound-increasing neuron with SST activation	Fig 2E	10 repeats	GLME	t_{laser}=0.33 t_{sound}=12.37 $t_{laser:sound}$=-8.34 DF = 206	p_{laser}=0.74 ***p_{sound}=1.2e-26** ***$p_{laser:sound}$=1.0e-14**	η_{laser}^2=2.3e-3 η_{sound}^2=0.84 $\eta_{laser:sound}^2$=0.78
VIP neuron with VIP activation	Fig 2F	10 repeats	GLME	t_{laser}=5.40 t_{sound}=0.93 $t_{laser:sound}$=-2.56 DF = 206	***p_{laser}=1.8e-7** p_{sound}=0.35 *$p_{laser:sound}$=1.1e-2**	η_{laser}^2=0.39 η_{sound}^2=2.8e-2 $\eta_{laser:sound}^2$=0.25
Sound-increasing neuron with VIP activation	Fig 2G	10 repeats	GLME	t_{laser}=2.45 t_{sound}=3.06 $t_{laser:sound}$=1.11 DF = 206	*p_{laser}=1.5e-2** **p_{sound}=2.5e-3** $p_{laser:sound}$=0.27	η_{laser}^2=0.12 η_{sound}^2=0.24 $\eta_{laser:sound}^2$=5.8e-2
FIGURE 3						
SST neurons with SST activation	Fig 3B	132 cells	GLME	t_{laser}=36.91 t_{sound}=1.32 $t_{laser:sound}$=0.16 DF = 27716	***p_{laser}=3.1e-291** p_{sound}=0.19 $p_{laser:sound}$=0.88	η_{laser}^2=0.14 η_{sound}^2=3.2e-4 $\eta_{laser:sound}^2$=6.7e-6
All non-SST neurons with SST activation	Fig 3C	2152 cells	GLME	t_{laser}=-1.27 t_{sound}=10.75 $t_{laser:sound}$=-6.35 DF = 451916	p_{laser}=0.20 ***p_{sound}=5.9e-27** ***$p_{laser:sound}$=2.2e-10**	η_{laser}^2=1.5e-5 η_{sound}^2=1.6e-3 $\eta_{laser:sound}^2$=8.5e-4

bioRxiv preprint doi: https://doi.org/10.1101/2023.02.01.526470; this version posted June 22, 2023. The copyright holder for this preprint (which was not certified by peer review) is the author/funder, who has granted bioRxiv a license to display the preprint in perpetuity. It is made available under aCC-BY-NC-ND 4.0 International license.

Sparseness with SST activation	Fig 3D	2152 cells	GLME	t_{laser}=3.39 DF = 6454	*****p_{laser}=7.1e-4**	η_{laser}^2=1.7e-3
Activity sparseness with SST activation	Fig 3E	13 populations	GLME	t_{laser}=3.20 t_{sound}=0.69 $t_{laser:sound}$=-0.99 DF = 230	****p_{laser}=1.6e-3** p_{sound}=0.49 $p_{laser:sound}$=0.33	η_{laser}^2=0.26 η_{sound}^2=9.8e-3 $\eta_{laser:sound}^2$=4.8e-2
VIP neurons with VIP activation	Fig 3G	226 cells	GLME	t_{laser}=41.50 t_{sound}=2.71 $t_{laser:sound}$=-1.96 DF = 47456	*****p_{laser}=0** ****p_{sound}=6.7e-3** ***$p_{laser:sound}$=4.95e-2**	η_{laser}^2=0.12 η_{sound}^2=9.3e-4 $\eta_{laser:sound}^2$=7.3e-4
All non-VIP neurons with VIP activation	Fig 3H	3095 cells	GLME	t_{laser}=34.18 t_{sound}=11.32 $t_{laser:sound}$=8.41 DF = 649946	*****p_{laser}=7.8e-256** *****p_{sound}=1.1e-29** *****$p_{laser:sound}$=4.1e-17**	η_{laser}^2=6.0e-3 η_{sound}^2=1.0e-3 $\eta_{laser:sound}^2$=8.4e-4
Sparseness with VIP activation	Fig 3I	3095 cells	GLME	t_{laser}=-22.95 DF = 9283	*****p_{laser}=2.2e-113**	η_{laser}^2=4.8e-2
Activity sparseness with VIP activation	Fig 3J	16 populations	GLME	t_{laser}=0.78 t_{sound}=-0.01 $t_{laser:sound}$=-0.49 DF = 284	p_{laser}=0.44 p_{sound}=0.99 $p_{laser:sound}$=0.62	η_{laser}^2=1.3e-2 η_{sound}^2=1.8e-6 $\eta_{laser:sound}^2$=8.2e-3
FIGURE 4						
Separation angle from 0dB at each laser power – SST activation	Fig 4D	15 angles, 13 recordings	GLME	t_{laser}=8.80 $t_{\Delta sound}$=12.37 $t_{laser:\Delta sound}$=-7.44 DF = 581	*****p_{laser}=1.6e-17** *****$p_{\Delta sound}$=2.3e-31** *****$p_{laser:\Delta sound}$=3.6e-13**	η_{laser}^2=0.30 $\eta_{\Delta sound}^2$=0.58 $\eta_{laser:\Delta sound}^2$=0.43
Separation angle from 0dB at each laser power – VIP activation	Fig 4F	15 angles, 16 recordings	GLME	t_{laser}=-2.75 $t_{\Delta sound}$=7.32 $t_{laser:\Delta sound}$=0.73 DF = 716	****p_{laser}=6.1e-3** *****$p_{\Delta sound}$=6.9e-13** $p_{laser:\Delta sound}$=0.47	η_{laser}^2=3.0e-2 $\eta_{\Delta sound}^2$=0.26 $\eta_{laser:\Delta sound}^2$=5.2e-3
Vector length at each laser power – SST activation	Fig 4H	21 lengths, 13 recordings	GLME	t_{laser}=-4.71 $t_{\Delta sound}$=5.71 $t_{laser:\Delta sound}$=-3.57 DF = 815	*****p_{laser}=2.9e-6** *****$p_{\Delta sound}$=1.6e-8** *****$p_{laser:\Delta sound}$=3.8e-4**	η_{laser}^2=6.1e-2 $\eta_{\Delta sound}^2$=0.16 $\eta_{laser:\Delta sound}^2$=9.1e-2
Vector length at each laser power – VIP activation	Fig 4J	21 lengths, 16 recordings	GLME	t_{laser}=2.50 $t_{\Delta sound}$=4.03 $t_{laser:\Delta sound}$=4.84 DF = 1004	***p_{laser}=1.2e-2** *****$p_{\Delta sound}$=6.1e-5** *****$p_{laser:\Delta sound}$=1.5e-6**	η_{laser}^2=9.7e-3 $\eta_{\Delta sound}^2$=4.8e-2 $\eta_{laser:\Delta sound}^2$=9.0e-2
FIGURE 5						
Sigmoid fit – offset – with SST activation	Fig 5D	None: 109 Med: 103 High: 64	GLME	t_{laser}=0.83 DF = 274	p_{laser}=0.41	η_{laser}^2=2.4e-3
Sigmoid fit – offset – with VIP activation	Fig 5D	None: 267 Med: 239 High: 269	GLME	t_{laser}=1.74 DF = 773	p_{laser}=8.1e-2	η_{laser}^2=3.6e-3

bioRxiv preprint doi: https://doi.org/10.1101/2023.02.01.526470; this version posted June 22, 2023. The copyright holder for this preprint (which was not certified by peer review) is the author/funder, who has granted bioRxiv a license to display the preprint in perpetuity. It is made available under aCC-BY-NC-ND 4.0 International license.

Sigmoid fit – range – with SST activation	Fig 5E	None: 109 Med: 103 High: 64	GLME	t_{laser}=-1.24 DF = 274	p_{laser}=0.22	η_{laser}^2=3.1e-3
Sigmoid fit – range – with VIP activation	Fig 5E	None: 267 Med: 239 High: 269	GLME	t_{laser}=3.11 DF = 773	****p_{laser}=1.9e-3**	η_{laser}^2=9.4e-3
Sigmoid fit – midpoint – with SST activation	Fig 5F	None: 109 Med: 103 High: 64	GLME	t_{laser}=2.65 DF = 274	****p_{laser}=8.6e-3**	η_{laser}^2=2.1e-2
Sigmoid fit – midpoint – with VIP activation	Fig 5F	None: 267 Med: 239 High: 269	GLME	t_{laser}=-0.88 DF = 773	p_{laser}=0.38	η_{laser}^2=5.9e-4
Sigmoid fit – width – with SST activation	Fig 5G	None: 109 Med: 103 High: 64	GLME	t_{laser}=-0.019 DF = 274	p_{laser}=0.99	η_{laser}^2=8.8e-7
Sigmoid fit – width – with VIP activation	Fig 5G	None: 267 Med: 239 High: 269	GLME	t_{laser}=0.56 DF = 773	p_{laser}=0.57	η_{laser}^2=2.2e-4
FIGURE 6						
Gaussian fit – offset – with SST activation	Fig 6D	None: 224 Med: 175 High: 130	GLME	t_{laser}=-3.16 DF = 527	****p_{laser}=1.7e-3**	η_{laser}^2=1.8e-2
Gaussian fit – offset – with VIP activation	Fig 6D	None: 243 Med: 278 High: 310	GLME	t_{laser}=0.71 DF = 829	p_{laser}=0.48	η_{laser}^2=5.3e-4
Gaussian fit – range – with SST activation	Fig 6E	None: 224 Med: 175 High: 130	GLME	t_{laser}=-5.41 DF = 527	*****p_{laser}=9.4e-8**	η_{laser}^2=3.8e-2
Gaussian fit – range – with VIP activation	Fig 6E	None: 243 Med: 278 High: 310	GLME	t_{laser}=5.60 DF = 829	*****p_{laser}=2.9e-8**	η_{laser}^2=1.7e-2
Gaussian fit – mean – with SST activation	Fig 6F	None: 224 Med: 175 High: 130	GLME	t_{laser}=0.35 DF = 527	p_{laser}=0.73	η_{laser}^2=1.9e-4
Gaussian fit – mean – with VIP activation	Fig 6F	None: 243 Med: 278 High: 310	GLME	t_{laser}=3.34 DF = 829	*****p_{laser}=8.6e-4**	η_{laser}^2=7.4e-3
Gaussian fit – standard deviation – with SST activation	Fig 6G	None: 224 Med: 175 High: 130	GLME	t_{laser}=-0.63 DF = 527	p_{laser}=0.53	η_{laser}^2=7.3e-4
Gaussian fit – standard deviation – with VIP activation	Fig 6G	None: 243 Med: 278 High: 310	GLME	t_{laser}=3.96 DF = 829	*****p_{laser}=8.1e-5**	η_{laser}^2=1.7e-2

bioRxiv preprint doi: https://doi.org/10.1101/2023.02.01.526470; this version posted June 22, 2023. The copyright holder for this preprint (which was not certified by peer review) is the author/funder, who has granted bioRxiv a license to display the preprint in perpetuity. It is made available under aCC-BY-NC-ND 4.0 International license.

Comparison	Figure	N	Test	Test Statistic	p-value	Effect size
SUPPLEMENTARY FIGURES						
FIGURE S2						
Control: VIP neurons with laser activation	Fig S2 A	54 cells	GLME	t_{laser}=1.27 t_{sound}=2.99 $t_{laser:sound}$=-0.11 DF = 11336	p_{laser}=0.20 **$**p_{sound}$=2.8e-3** $p_{laser:sound}$=0.91	η_{laser}^2=6.5e-4 η_{sound}^2=5.5e-3 $\eta_{laser:sound}^2$=1.1e-5
Control: All neurons (VIP excluded) with laser activation	Fig S2 B	492 cells	GLME	t_{laser}=0.46 t_{sound}=12.23 $t_{laser:sound}$=3.27 DF = 103316	p_{laser}=0.64 **$***p_{sound}$=2.1e-34** **$**p_{laser:sound}$=1.1e-3**	η_{laser}^2=8.5e-6 η_{sound}^2=9.0e-3 $\eta_{laser:sound}^2$=9.8e-4
FIGURE S3						
SST: Decoding accuracy of a linear SVM decoder with laser activation	Fig S3 A	13 populations	GLME	t_{laser}=-3.92 t_{sound}=-2.84 $t_{laser:sound}$=1.92 DF = 269	**$***p_{laser}$=1.11e-4** **$**p_{sound}$=0.0049** $p_{laser:sound}$=0.056	η_{laser}^2=0.19 η_{sound}^2=0.16 $\eta_{laser:sound}^2$=0.11
VIP: Decoding accuracy of a linear SVM decoder with laser activation	Fig S3 B	13 populations	GLME	t_{laser}=-0.69 t_{sound}=-3.58 $t_{laser:sound}$=-0.11 DF = 332	p_{laser}=0.49 **$***p_{sound}$=3.99e-4** $p_{laser:sound}$=0.91	η_{laser}^2=4.3e-3 η_{sound}^2=0.15 $\eta_{laser:sound}^2$=2.7e-4
FIGURE S4						
Activity sparseness from 0dB and no laser power with SST activation	Fig S4 A	13 populations	GLME	t_{laser}=1.60 t_{sound}=1.17 $t_{laser:sound}$=-1.54 DF = 230	p_{laser}=0.11 p_{sound}=0.24 $p_{laser:sound}$=0.12	η_{laser}^2=5.5e-2 η_{sound}^2=1.9e-2 $\eta_{laser:sound}^2$=7.7e-2
Activity sparseness from 0dB and no laser power with VIP activation	Fig S4 B	16 populations	GLME	t_{laser}=-3.52 t_{sound}=-0.49 $t_{laser:sound}$=0.0059 DF = 284	**$***p_{laser}$=4.9e-4** p_{sound}=0.62 $p_{laser:sound}$=0.995	η_{laser}^2=0.15 η_{sound}^2=2.1e-3 $\eta_{laser:sound}^2$=7.6e-7

Mouse strains and numbers

Experiment	Figures	Strain	Number of mice	Number of recordings
GCaMP7f + ChrimsonR	Figs 2-6	CDH23 x VIP-Cre	2	7
		CDH23 x SST-Cre	5	13
GCaMP6m + ChrimsonR	Figs 2-6	CDH23 x VIP-Cre	2	9
		CDH23 x SST-Cre	0	0

bioRxiv preprint doi: https://doi.org/10.1101/2023.02.01.526470; this version posted June 22, 2023. The copyright holder for this preprint (which was not certified by peer review) is the author/funder, who has granted bioRxiv a license to display the preprint in perpetuity. It is made available under aCC-BY-NC-ND 4.0 International license.

Control: GCaMP7f + Flex.tdTomato – VIP cells	Fig S2A	CDH23 x VIP-Cre	4	7
Control: GCaMP7f + Flex.tdTomato – Non-VIP cells	Fig S2B	CDH23 x VIP-Cre	2	4